

Template-Directed Formation of Hemispherical Cavities of Varying Depth and Diameter in a Silicate Matrix Prepared by the Sol–Gel Process

Mandakini Kanungo, P. N. Deepa, and Maryanne M. Collinson*

Department of Chemistry, Kansas State University, Manhattan, Kansas 66506-3701

Received May 9, 2004. Revised Manuscript Received August 25, 2004

2-D ordered arrays of hemispherical cavities were formed in a sol–gel-derived silicate film on a glassy carbon electrode using polystyrene latex spheres as templates. The depth and the diameter of the cavities were varied over 1 order of magnitude by changing the diameter of the template and diluting the sol. Sulfate-stabilized polystyrene latex spheres ranging in size from 100 to 1000 nm were doped into a silica sol prepared from the hydrolysis and condensation of tetramethoxysilane, and the resultant solution was spin cast on a glassy carbon electrode. The 2-D ordered array of spheres in a thin silicate film was removed via soaking the film in chloroform. Scanning electron microscopy and atomic force microscopy (AFM) were used to image the films, and AFM with high-resolution TM tips was used to measure the depth and diameter of the cavities. The cavities are open at the top and bottom and provide direct access to the underlying electrode surface as verified by cyclic voltammetry. Nanosized copper and polyaniline were electrodeposited in the cavities after pinholes were “capped” to create an ordered array of conducting nanostructures in a templated silica host.

Introduction

Nanostructured materials have many uses in chemistry and material science that range from catalytic supports to chemical sensors to molecular sieving.^{1–3} Among various strategies for the preparation of microporous ($d < 2$ nm), mesoporous ($2 \text{ nm} < d < 50$ nm), and macroporous ($d > 50$ nm) materials, template-based sol–gel processing has rapidly gained popularity.⁴ In this approach, a template is added to a sol (e.g., that obtained from the hydrolysis and condensation of silicon or titanium alkoxides⁵). Upon gelation, the matrix forms around the template.⁴ After the template is removed, cavities of the same shape and size as the template remain in the host.⁴ Examples of templates that have been used include small molecules,⁶ dendrimers,⁷ organic functional groups,⁸ bridged organic ligands,^{9,10} surfactant assemblies,^{11,12} and latex spheres.^{13–26}

Thin sol–gel-derived films have seen many more applications in chemical sensing^{27–29} as compared to sol–gel-derived monoliths because the path length for the diffusion of reagents to the underlying surface is on the order of a few hundred nanometers. However, while monoliths can be 40–70% porous,⁵ thin films can be significantly less porous due in part to the overlap of gelation/drying that occurs due to their fabrication procedure (spin coating or dip coating).⁸ The use of templates provides one means to increase the porosity of these materials and increases the accessibility of

- (1) Bayley, H.; Martin, C. R. *Chem. Rev.* **2000**, *100*, 2575–2594.
- (2) Beecroft, L. L.; Ober, C. K. *Chem. Mater.* **1997**, *9*, 1302–1317.
- (3) Schollhorn, R. *Chem. Mater.* **1996**, *8*, 1747–1757.
- (4) Raman, N. K.; Anderson, M. T.; Brinker, C. J. *Chem. Mater.* **1996**, *8*, 1682–1701.
- (5) Brinker, J.; Scherer, G. *Sol–Gel Science*; Academic Press: New York, 1989.
- (6) Makote, R.; Collinson, M. M. *Chem. Mater.* **1998**, *10*, 2440–2445.
- (7) Larsen, G.; Lotero, E.; Marquez, M. *Chem. Mater.* **2000**, *12*, 1513–1515.
- (8) Lu, Y.; Cao, G.; Kale, B. P.; Prabakar, S.; Lopez, G. P.; Brinker, C. J. *Chem. Mater.* **1999**, *11*, 1223–1229.
- (9) Chevalier, P.; Corriu, R. J. P.; Delord, P.; Moreau, J. J. E.; Man, M. W. C. *New J. Chem.* **1998**, 423–433.
- (10) Loy, D. A.; Carpenter, J. P.; Alam, T. M.; Shaltout, R.; Dorhout, P. K.; Breaves, J.; Small, J. H.; Shea, K. J. *J. Am. Chem. Soc.* **1999**, *121*, 5413–5425.
- (11) Beck, J. S.; Vartuli, J. C.; Roth, W. J.; Leonowicz, M. E.; Kresge, C. T.; Schmitt, K. D.; Chu, C. T.-W.; Olson, D. H.; Sheppard, E. W.; McCullen, S. B.; Higgins, J. B.; Schlenker, J. L. *J. Am. Chem. Soc.* **1992**, *114*, 10834–10843.

- (12) Kresge, C. T.; Leonowicz, M. E.; Roth, W. J.; Vartuli, J. C.; Beck, J. S. *Nature* **1992**, *359*, 710–712.
- (13) Hotta, Y.; Alberius, P. C. A.; Bergstrom, L. *J. Mater. Chem.* **2003**, *13*, 496–501.
- (14) Caruso, F.; Caruso, R. A.; Mohwald, H. *Science* **1998**, *282*, 1111–1114.
- (15) Caruso, F.; Shi, X.; Caruso, R. A.; Susha, A. *Adv. Mater.* **2001**, *13*, 740–744.
- (16) Jiang, P.; Bertone, J. F.; Hwang, K. S.; Colvin, V. L. *Chem. Mater.* **1999**, *11*, 2132–2140.
- (17) Jiang, P.; Hwang, K. S.; Mittleman, D. M.; Bertone, J. F.; Colvin, V. L. *J. Am. Chem. Soc.* **1999**, *121*, 11630–11637.
- (18) Johnson, S. A.; Ollivier, P. J.; Mallouk, T. E. *Science* **1999**, *283*, 963–965.
- (19) Park, S. H.; Xia, Y. *Adv. Mater.* **1998**, *10*, 1045–1048.
- (20) Park, S. H.; Xia, Y. *Langmuir* **1999**, *15*, 266–273.
- (21) Valtchev, V. *Chem. Mater.* **2002**, *14*, 956–958.
- (22) Valtchev, V. *Chem. Mater.* **2002**, *14*, 4371–4377.
- (23) Yu, A.; Meiser, F.; Cassagneau, T.; Caruso, F. *Nano Lett.* **2004**, *4*, 177–181.
- (24) Velev, O. D.; Kaler, E. W. *Adv. Mater.* **2000**, *12*, 531–534.
- (25) Xia, Y.; Gates, B.; Yin, Y.; Lu, Y. *Adv. Mater.* **2000**, *12*, 693–713.
- (26) Yi, G.-R.; Moon, J. H.; Yang, S.-M. *Chem. Mater.* **2001**, *13*, 2613–2618.
- (27) Avnir, D. *Acc. Chem. Res.* **1995**, *28*, 328–334.
- (28) Dave, B. C.; Dunn, B.; Valentine, J. S.; Zink, J. I. *Anal. Chem.* **1994**, *66*, 1120A–1127A.
- (29) Lev, O.; Tsionsky, M.; Rabinovich, L.; Glezer, V.; Sampath, S.; Pankratov, I.; Gun, J. *Anal. Chem.* **1995**, *67*, 22A–30A.

reagents that may be entrapped into this “porous” network. Under the right conditions, these template-induced cavities can also be used as “templates” to grow nanosized metals or polymers within a porous network.

In previous work, we have demonstrated the utility of using polystyrene latex spheres as templates to create nanosized cavities into a silicate thin film prepared by the sol–gel process.^{30,31} In our first report, we had at best 10^7 ca. 300 nm diameter holes/cm² randomly dispersed in a silicate film that were open at both the top and the bottom, thus exposing the underlying surface.³¹ In a recent communication, we have demonstrated how the number of the cavities in the film can be increased by 2 orders of magnitude by packing the spheres in a closely packed array and how it is possible to vary their depth over a limited region by diluting the sol.³⁰ In this work, we provide more details about how the depth and diameter of the nanosized cavities in the silica host can be varied over 1–2 orders of magnitude by (1) changing the size of the sphere and (2) diluting the sol. We also show for the first time how the cavities can be used as templates to synthesize ordered arrays of nanosized particles of metal and conducting polymer. By controlling both the size of the template as well as the composition of the sol, an ordered array of cavities of a multitude of sizes can be created in a thin silica framework.

Experimental Section

Reagents and Equipment. Tetramethoxysilane (TMOS, 99%), *n*-octyltrimethoxysilane, sodium dodecyl sulfate (SDS, 98%), and ferrocene methanol (97%) were purchased from Aldrich. Chloroform, hydrochloric acid, aniline, and sulfuric acid were purchased from Fisher Scientific. Aqueous suspensions of polystyrene microspheres (PSMS) with diameters ranging from 0.1 to 1 μ m were obtained from Interfacial Dynamics Corp. (Portland, OR) (8.2 wt/v %, surfactant free, sulfated). Water was purified to Type I using a Labconco water proPS four-cartridge system. Aniline was distilled under reduced pressure and stored under nitrogen.

Electrochemical experiments were performed using a BAS CV-50W voltammetric analyzer using a one-chamber three-electrode cell. The working electrode consists of a glassy carbon electrode (5 mm diameter, area = 0.2 cm²). The reference and auxiliary electrodes were an Ag/AgCl electrode (1 M KCl) and a platinum wire electrode, respectively. Atomic force microscopy (AFM) measurements were performed in both the contact mode and the tapping mode with a Nanoscope IIIa multimode SPM microscope (Digital Instruments, Inc. Santa Barbara, CA). Contact mode experiments were performed with a microfabricated silicon nitride tip at a scan rate of 1–3 Hz. Tapping mode experiments were performed using a high aspect ratio tip (Veeco Nanoprobe tips, model # TESP-HAR) using a scan rate of 0.5–1 Hz. SEM images were collected with a Hitachi scanning electron microscope S-3500 N equipped with an Oxford detector for energy-dispersive X-ray analysis. The samples were sputter coated with a thin layer of gold to reduce charging effects.

Procedures. Sols with Si:H₂O ratios of 1:9, 1:31, 1:43, and 1:430 were prepared by mixing the appropriate amount of TMOS (1.5, 0.65, 0.5, 0.05 mL, respectively), 2.3 mL of water (except for the 1:9 sol, which was 1.3 mL), 2.4 mL of methanol, and 0.3 mL of 0.1 M hydrochloric acid followed by stirring for 30 min. The pH of each sol was measured with short-range

pH paper and found to be identical. Polystyrene latex spheres (PS, 0.100, 0.340, 0.530, and 0.960 μ m diameter) were sonicated 5–10 min before use. The aged (2 days) silica sol was then added to a PS suspension in a ratio of 1:1 (v/v). Prior to the addition of the latex spheres, 5 mM SDS was added to improve the wettability of the sol so that it can better coat the glassy carbon substrate (5 mm diam, Alfa) used in this work. The PS-doped silica sol was then spin cast on a glassy carbon substrate at ca. 3000 rpm using an in-house built rotator. Prior to the spin casting procedure, the glassy carbon was polished with 0.05 μ m alumina particles on a napless polishing cloth (Buehler), sonicated in water for 10–15 min, and then dried. The thin films were allowed to dry overnight at ca. 30–35% RH, room temperature. The films were soaked in chloroform for 2–3 h to remove the polystyrene spheres. In some experiments, the apparent “pinholes” in the PS-doped silicate films were blocked by immersing the film in a dilute solution of *n*-octyltrimethoxysilane (5% in dry methanol) for 2 h. The films were rinsed with methanol to remove the excess silica and were dried at room temperature. The films were put in chloroform to extract the polystyrene spheres as described above.

Results and Discussion

Preparation. A 2-D ordered monolayer of polystyrene latex spheres can be formed on a polished glassy carbon substrate by simply mixing the latex spheres with a surfactant-doped silica sol followed by spin coating.^{19,20} In this work, the size of the latex spheres was varied from 100 to 1000 nm in diameter, and the sol was diluted by increasing the amount of water relative to silica. Regardless of the size of the spheres or the water content in the sol, the spheres predominantly pack in a hexagonal close-packed array. Both SEM and AFM have been used to “visualize” the materials, and similar results were obtained with both microscopic methods. Figure 1 shows typical SEM images of 500 nm diameter spheres packed in a silicate film in a closely packed array. While the packing arrangement is not perfect due in part to imperfections and scratches on the glassy carbon surface, there are large areas that are distinctly ordered. AFM images show nearly identical results.

The sizes of the defect-free areas range from 1 to greater than 100 μ m² depending on the smoothness of

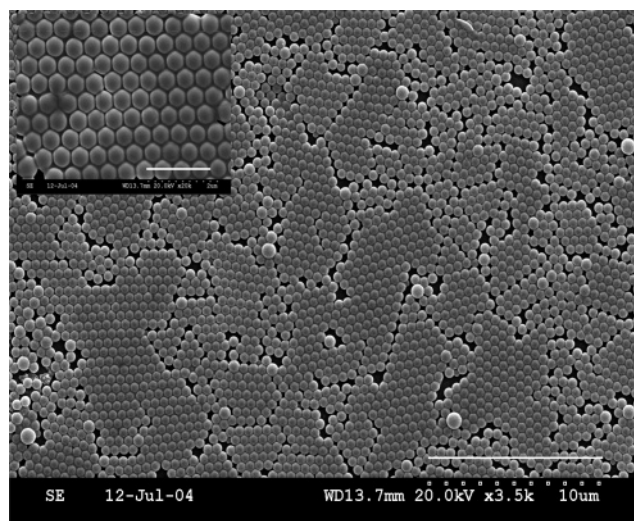


Figure 1. SEM images of 500 nm diameter latex spheres embedded in a silicate film on a glassy carbon substrate. The silica sol had a Si:H₂O mole ratio of 1 to 43. The scale bar is 10 μ m in the full image and 2 μ m in the inset.

(30) Kanungo, M.; Collinson, M. M. *Chem. Commun.* **2004**, 5, 548–549.

(31) Khramov, A. N.; Munos, J.; Collinson, M. M. *Langmuir* **2001**, 17, 8112–8117.

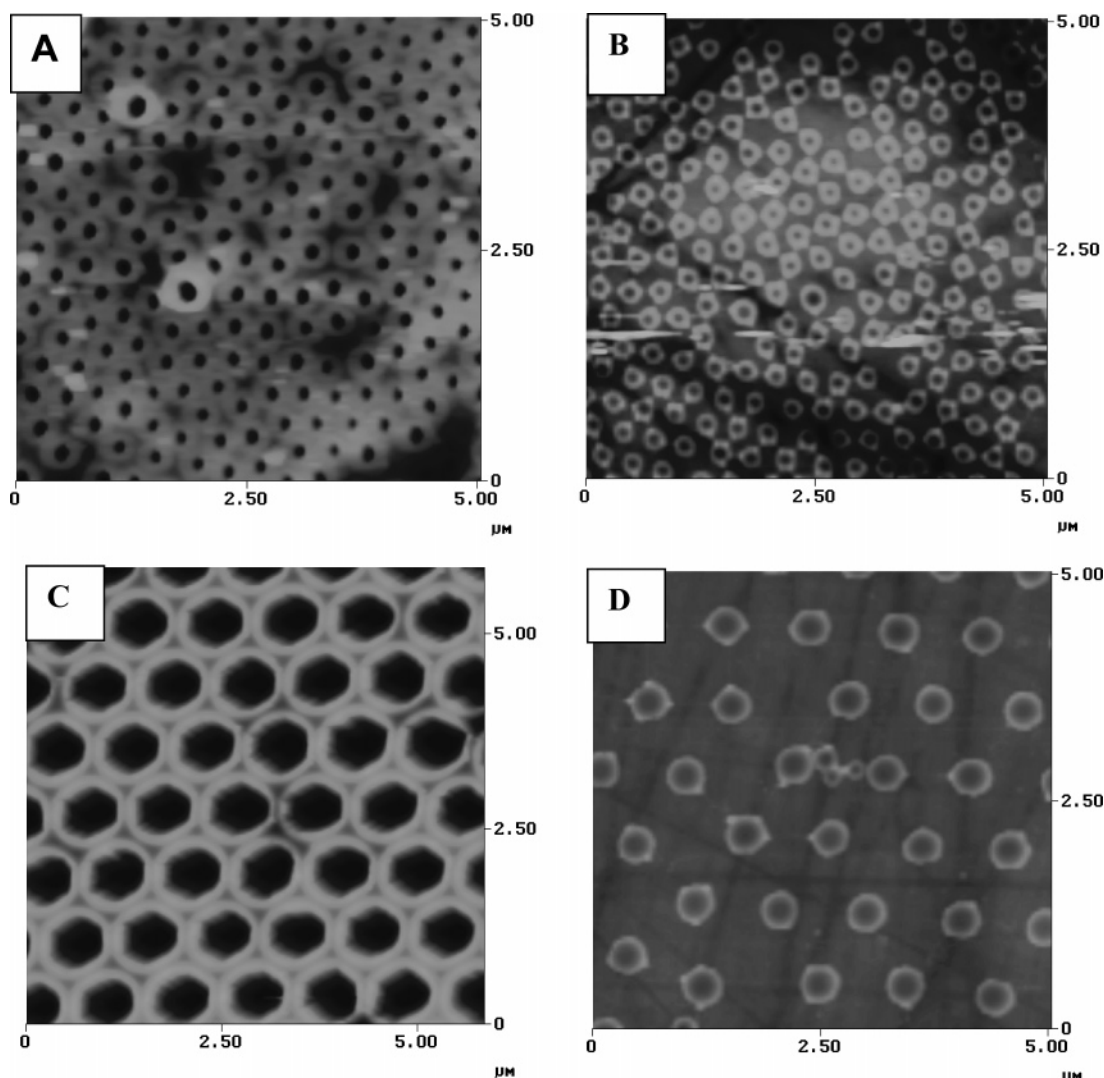


Figure 2. $5\ \mu\text{m} \times 5\ \mu\text{m}$ AFM images of cavities formed in a silicate film after the 300 nm diameter (A,B) and the 1000 nm diameter (C,D) spheres were removed from the film. The Si:H₂O mole ratio of the sol used to make the films was 1:9 (A,C) and 1:430 (B,D). The full gray scale image is 500 nm (1000 nm diam spheres) or 200 nm (300 nm diam spheres).

the substrate and the diameter of the spheres. Naturally, as the diameter of the latex spheres is reduced, the size of the defect-free area decreases. For the 100 nm diameter spheres, the defect-free area was approximately $1\ \mu\text{m}^2$, whereas for spheres that were $10\times$ as large, the area was greater than $100\ \mu\text{m}^2$. The number of particles in a square centimeter agrees with that predicted for a closely packed array. It ranges from 10^8 to 10^{10} cavities per cm^2 for the 1000 and 100 nm diameter spheres, respectively.

Several methods can be used to remove the spheres from the silicate matrix. Calcination has been shown to be an effective method to remove a template from an inorganic host. However, if one wants to preserve the underlying surface (in this case, carbon), this method will not work. A milder chemical treatment obtained by soaking the templated film in either chloroform or toluene for 2+ h is milder. Figure 2 shows AFM images of an ordered arrangement of cavities formed in a silicate matrix using 300 and 1000 nm diameter spheres as the template. In this case, the sol was prepared with a Si:H₂O mole ratio of 1:9 (Figure 2A,C) or with a ratio of 1:430 (Figure 2B,D).

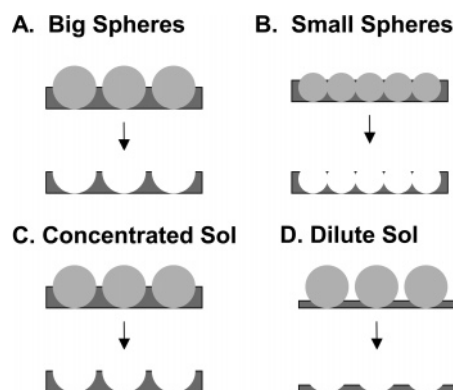


Figure 3. Cartoon depicting how the depth and diameter of the cavities can be changed by varying the size of the template and/or the sol composition.

As can be seen in both images, the cavities are in an ordered arrangement even after chloroform treatment consistent with that observed for the spheres before treatment. In a 2D-format, the AFM images look like they are composed of “donuts” packed in an ordered arrangement (Figure 2), whereas in a 3D AFM format

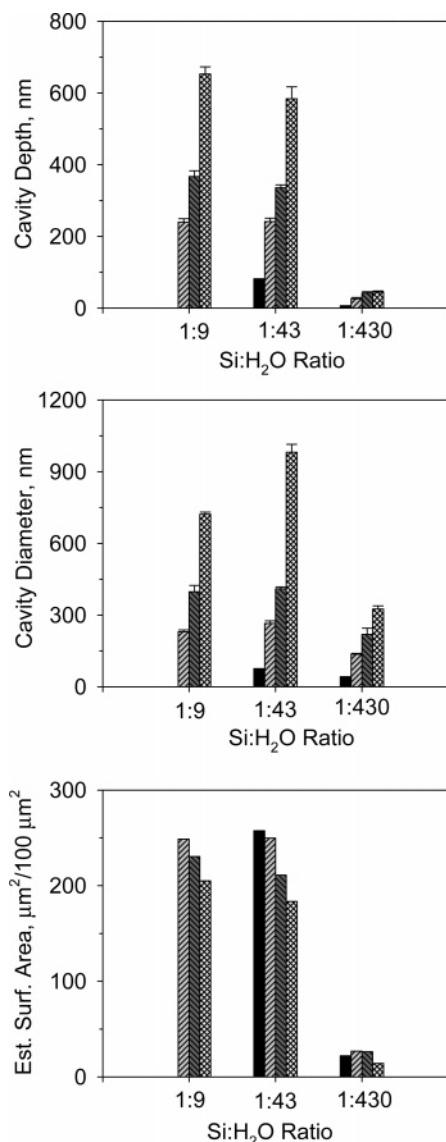


Figure 4. Variation in the top diameter, depth, and estimated surface area of the cavities in a silicate film as a function of the Si:H₂O mole ratio used to make the sol. From left to right, spheres were 100 (1:43, 1:430 only), 300, 500, and 1000 nm in diameter.

they look like “volcanoes”. As noted before for our “randomly dispersed” cavities, there is a “ridge” of silica around each particle due to the wetting of the sulfate-stabilized polystyrene sphere by the sol.³¹

Characterization. One goal of this work was to demonstrate how easy it is to vary the depth and diameter of cavities formed in a silicate film through both (1) changes in the size of the template and (2) changes in the sol–gel processing conditions. Tuning the depth and diameter of the cavities allows the surface area and the porosity of the film to be varied. If one were interested in these materials as chemical sensors, it would be desirable to have a large number of cavities with a large fraction of the matrix exposed. If one were interested in using these materials as “templates” to grow nanostructures, it would be desirable to be able to vary the dimensions of the cavity from large to small.

Figure 3 shows a cartoon depicting how the diameter and depth of the cavities can be changed via modifica-

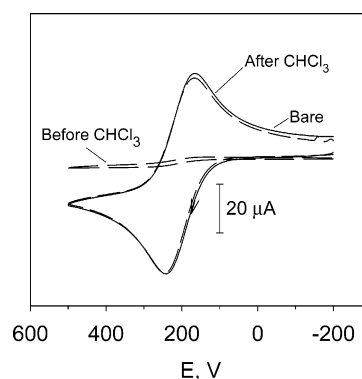


Figure 5. Cyclic voltammograms of 1 mM ferrocene methanol in 0.10 M KCl at a bare electrode, a “capped” templated electrode before chloroform, and a “capped” templated electrode after chloroform treatment. Scan rate: 100 mV/s. The template had a diameter of 500 nm, and a sol with a Si:H₂O of 1:43 was used.

tion in the diameter of the sphere and the sol–gel processing conditions. It is straightforward to understand how the cavity dimensions can be changed by varying the size of the template (Figure 3A,B). A bigger template results in a bigger hole, whereas a smaller template results in a smaller hole. It is also just as easy to just pick one size sphere and dilute the sol with water relative to silica while keeping pH approximately constant. If the sol has a small H₂O:Si ratio (not diluted), “thick” films will be formed that will result in deep cavities in the silicate matrix once the template is removed. If the sol has a high H₂O:Si ratio (diluted), “thin” films will be obtained that produce cavities that are very shallow in depth and relatively small in diameter once the template is removed. It may also be possible to change silica film thickness by changing the pH of the sol while keeping other variables constant as recently shown by Hotta et al.¹³ In our work, however, the pH values of the sols were the same.

Upon further examination of Figure 2, it may appear that the cavities formed in the film prepared with a Si:H₂O mole ratio of 1:9 are further apart than those prepared from 1:430, but they are not. The center-to-center distance between cavities is still approximately equal to the size of the latex sphere; only the ones produced from the diluted sol are shallower. By playing around with the size of the template and composition of the sol, we could vary the dimensions of the cavities several orders of magnitude. In this study, the focus has been on spheres ranging in diameter from 100 to 1000 nm, but other sizes could be used as well.

To properly image the depth and top diameter of cavities, it is extremely important to use a sharp high-resolution tapping mode tip. From line scan images obtained with such a tip, it is possible to estimate both the depth and the diameter of the cavities as a function of the size of the template used and the Si:H₂O mole ratio in the sol. Figure 4 shows a bar chart depicting the depth and diameter of the cavities as a function of both size and sol composition. By manipulating both variables, the depth has been changed from ca. 7 to 650 nm and the diameter has been changed from 40 to 1000 nm.

If each cavity is modeled as a “spherical cap” or a “spherical segment”³² as it is mathematically termed,

the surface area can be calculated from the formula

$$SA = 2\pi rh \times \text{\#cavities}/100 \mu\text{m}^2$$

where r is the radius of the sphere and h is the depth of the cavity. Figure 4C shows how the surface area can be significantly changed. If it is assumed that the film has no internal porosity, then the total surface area of the film (cavities plus area surrounding the cavities) increases by a factor of 3–4 by having a close-packed array of cavities in the film. The film, however, does have some internal porosity, but this is hard to quantify due to the small amounts of material on a surface. What is more important, however, is that a greater fraction of this internal porosity is exposed once the spheres are removed from the silicate film. If a reagent or receptor is trapped within the silicate framework, it will be more

readily accessible to an analyte in solution. In principle, this should increase the sensitivity of the sol–gel-derived sensor as well as increase its response time.

Template-Directed Synthesis. One of the major advantages of casting the silicate film on an electrode surface is that it provides a means to conduct electrochemistry within these nanosized cavities. As indicated in prior work, the cavities are open at the top as well as on the bottom, thus exposing the underlying electrode surface. The size of the exposed area is difficult to precisely measure, but it appears to be on the order of 50–100 nm, at least for the 500 nm diameter spheres.³¹ When the spheres are far apart and just randomly dispersed on the surface, electrochemistry can easily be done solely in the exposed cavities as there are no pinholes in the silicate matrix that allow a redox species direct access to the underlying electrode surface.³¹

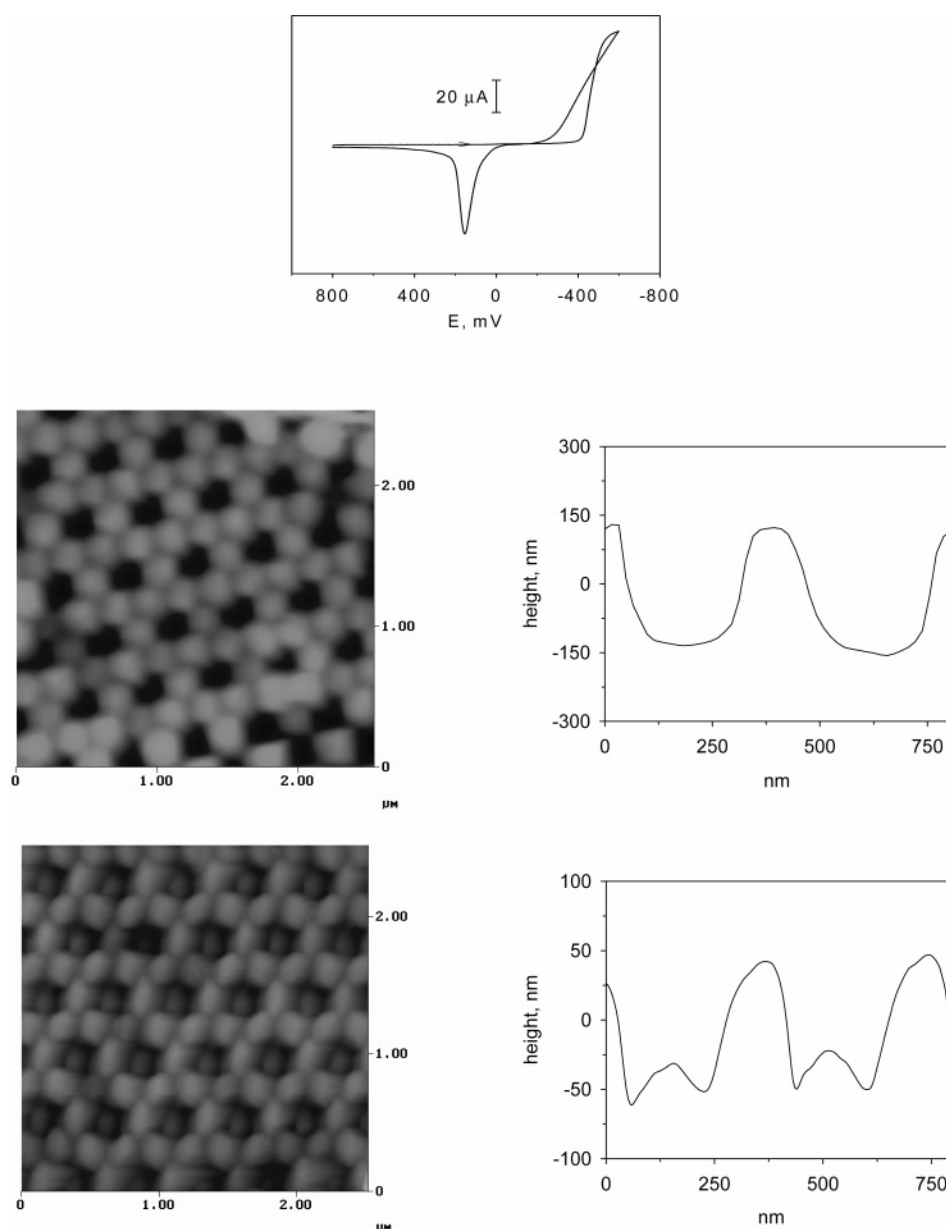


Figure 6. Top: CV of 5 mM CuSO_4 in 0.1 M H_2SO_4 at a “capped” templated electrode (10 mV/s). Bottom: $2.5 \times 2.5 \mu\text{m}$ AFM images and line scans recorded with a high aspect ratio tapping mode tip of a “capped” templated film before and after application of -0.2 V for 50 s. The template had a diameter of 500 nm, and a sol with a Si: H_2O of 1:43 was used. The full gray scale image is 300 nm.

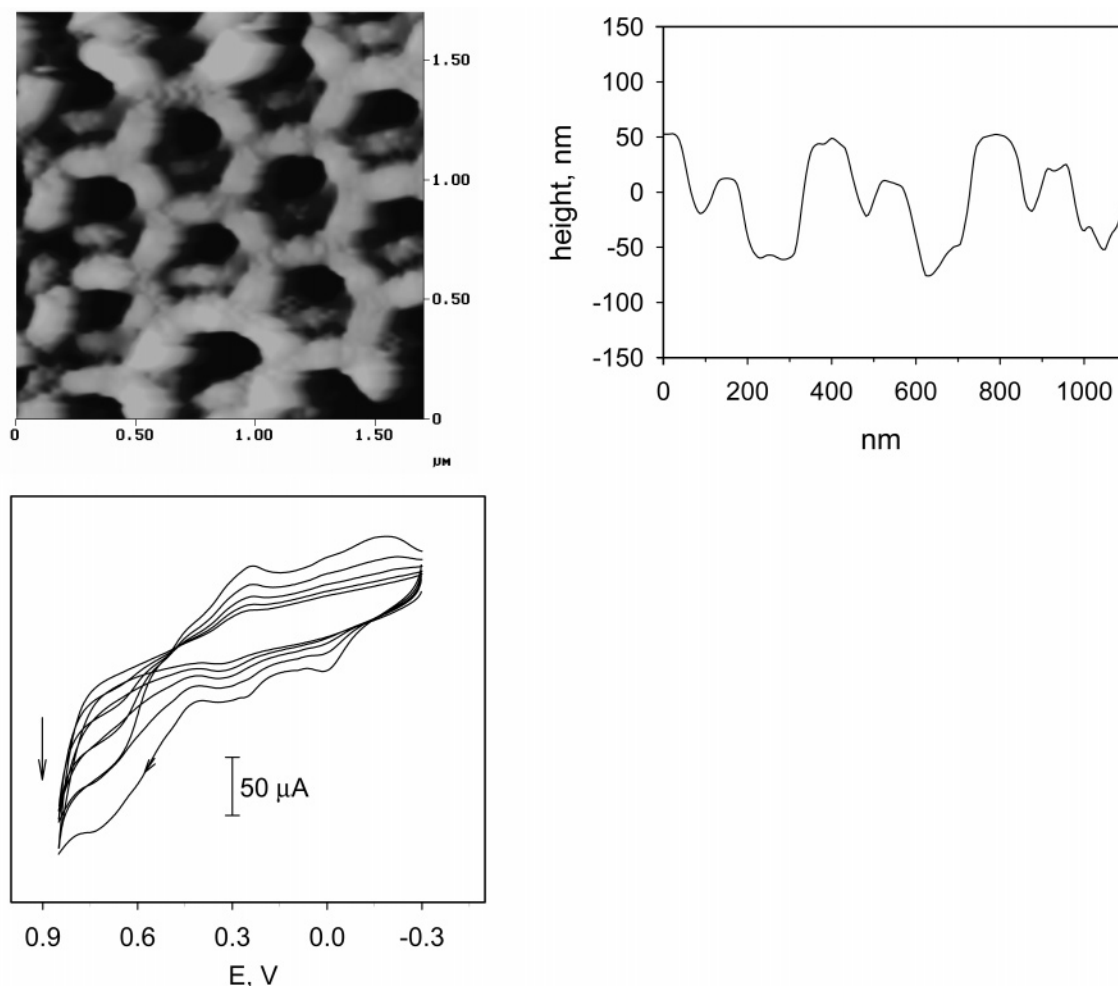


Figure 7. AFM images and line scans recorded with a high aspect ratio tapping mode tip of a “capped” templated film after the electrodeposition (CV acquired at 50 mV/s) of polyaniline from a 0.1 M polyaniline in 0.5 M H₂SO₄. The template had a diameter of 500 nm, and a sol with a Si:H₂O of 1:43 was used. The full gray scale image is 300 nm.

However, when the spheres are arranged in a closely packed arrangement, pinholes develop between spheres and at dislocations in the film.

Figure 5 shows a cyclic voltammogram (CV) of 1 mM ferrocene methanol at a bare glassy carbon surface. The electrochemical response of an electrode that has a film containing a closely packed array of spheres (before chloroform treatment) embedded in a silicate framework looks identical to this CV (CV not shown). The silicate film obviously has a large number of pinholes that are closely spaced together such that the diffusion layer of ferrocene methanol overlaps.³³ Under this condition, the surface appears as one big electrode.³³

To do electrochemistry predominantly in the cavities, it is necessary to “plug” these pinholes. To do this, one must soak the sphere-coated silicate film (before cavity removal) in an alcoholic solution of octyltrimethoxysilane for a few hours. The long-chain hydrophobic silane reacts with the exposed silica surface, blocking many of the “nanosized” holes present in the film. We have also tried spin coating a diluted, undoped silica sol on top of the film containing the spheres, but this was

shown to be less effective than the use of the organoalkoxysilane.

Figure 5 shows a CV of ferrocene methanol at a film that has been capped with the spheres present. As can be seen, the electrochemical response is significantly reduced. The CV has a sigmoidal appearance, indicating that there are still pinholes remaining in the films, but they are small and relatively far apart and behave like an ultramicroelectrode.³³ Now, when the spheres are subsequently removed from the modified film, access to the underlying electrode surface is predominantly through the cavity as most of the pinholes remain capped by the organic layer. Figure 5 shows a CV of ferrocene methanol at such a film. Once again, it looks like that expected for a bare electrode and corresponds to the “total overlap regime”. Because the cavities are shallow as compared to the thickness of the diffusion layer and because they are close together relative to the thickness of the diffusion layer, the electrochemical response of the film looks identical to the bare electrode at all sweep rates (2–1000 mV/s).

One motivation for this work was to demonstrate how these materials can be used as “templates” to grow nanostructures within each cavity. We evaluated the feasibility for doing this via the electrodeposition of copper and the conducting polymer, polyaniline. Bartlett

(32) See <http://mathworld.wolfram.com/sphericalcap.html>.

(33) Wightman, R. M.; Wipf, D. O. *Voltammetry at Ultramicroelectrodes*; Marcel Dekker: New York, 1989; Vol. 15, pp 267–353.

and co-workers have previously described how gold and platinum can be electrodeposited in the interstitial spaces between latex spheres assembled on a gold electrode to prepare a structured metal film.^{34,35} In this work, the interstitial spaces between spheres (cavities) are filled with silica except at the very bottom of the cavity.

Figure 6 shows AFM images obtained for a film prepared from 500 nm diameter spheres before and after electrodeposition of copper. The top image and line scan obtained with a high-resolution TM-AFM tip shows the cavities in the film just before deposition (after capping and sphere removal). The depth of the cavities increases only slightly after capping. The bottom image and line scan show the cavities after a reducing potential has been applied to the templated electrode immersed in an acidic solution of copper sulfate for 50 s. Both the line scan and the image show that something has been deposited in the cavities. The size of the deposit depends on the electrodeposition time: longer times result in bigger deposits and vice versa. The shape of the CV is characteristic of copper electrodeposition on the conducting surface.

SEM was also used to visualize the films. In large-scale images, it was difficult to visually see the nanosized deposits deep within the nanoscale cavities because they are so small and located >100 nm below the surface. The presence of globules between cavities, however, was observed in some areas. This is expected as the voltammetry (Figure 5) indicates that there are pinholes in the film where copper can be electrochemically reduced. EDAX analysis confirms that copper is present inside the cavity and that the deposits observed between cavities in some areas are also copper. It may be possible to improve the capping procedure by optimizing the experimental conditions (humidity, soaking time, concentration, and type of silane).

Conducting polymers can also be deposited in each cavity as well using a similar procedure. Figure 7 shows the AFM image of the cavities after capping and sphere removal. The templated film is placed in 0.1 M aniline in 0.5 M H₂SO₄, and the electrode potential is electrochemically cycled five times. As can be seen in the AFM image and its corresponding line scan, polyaniline has formed in each cavity. Future work will explore the feasibility of removing the silicate film without destroying the metal/polymer and controlling the size and spacing of the nanostructures via changes in the size and depth of the cavity.

In some respects, these templated films may be reminiscent of the "track-etch" or alumina membrane electrodes popularized by the Martin group^{36–38} or the microhole electrodes described by Morita and Shimizu.^{39–41} Both provide a means to fabricate an array of "nanosized" electrodes, and both provide a means to physically control the growth of metal nanostructures or conducting polymers. However, the cavities described herein are not very deep (nm vs μ m) and thus provide a means of forming smaller nanostructures on surfaces. In addition, the sol–gel-derived network surrounding the polystyrene templated cavities is porous, opening up the possibility of increasing the access to reagents that may be trapped within the matrix.

Conclusions

2-D ordered arrays of hemispherical shaped nanosized cavities of almost any diameter and depth can be formed into a sol–gel-derived silicate framework by templating with polystyrene latex spheres. While this work focused on the creation of cavities with depths and diameters in the 10's to 100's of nanometers, the use of spheres ranging in size from 20 nm to 10 μ m (commercially available) coupled with variations in the sol will significantly extend this range from nanometers to micrometers. In this work, shallow cavities (\sim 10 nm) were made using small spheres (100 nm) and a diluted sol, whereas larger, deeper cavities (\sim 600 nm) were made by using large spheres (1000 nm) and a more conventional sol. One very promising feature of these materials is that the cavities are open at the bottom and top, providing access to the underlying surface. When the polystyrene latex sphere-doped sol is cast on a conducting surface, an array of ultramicroelectrodes is formed upon removal of the latex spheres. Conducting polymers or metals can be electrochemically deposited in each cavity provided pinholes in the film are first blocked with an organosilane. These thin porous materials have many possible applications in the areas of chemical sensing and template-directed synthesis of conducting nanostructures. Future work will involve the exploration of some of these ideas.

Acknowledgment. We gratefully acknowledge support of this work by the National Science Foundation (CHE, DMR-IMR). We would also like to thank Kent Hampton for the acquisition of the SEM images.

CM049270X

(34) Abdelsalam, M. W.; Bartlett, P. N.; Baumberg, J. J.; Coyle, S. *Adv. Mater.* **2004**, *16*, 90–93.

(35) Bartlett, P. N.; Baumberg, J. J.; Birkin, P. R.; Ghanem, M. A.; Netti, M. C. *Chem. Mater.* **2002**, *14*, 2199–2208.

(36) Martin, C. R. *Acc. Chem. Res.* **1995**, *28*, 61–68.

(37) Martin, C. R. *Science* **1994**, *266*, 1961–1966.

(38) Martin, C. R. *Chem. Mater.* **1996**, *8*, 1739–1746.

(39) Morita, K.-I.; Shimizu, Y. *Anal. Chem.* **1989**, *61*, 159–162.

(40) Shimizu, Y.; Morita, K.-I. *Anal. Chem.* **1990**, *62*, 1498–1501.

(41) Tokuda, K.; Morita, K.-I.; Shimizu, Y. *Anal. Chem.* **1989**, *61*, 1763–1766.